



# STRUCTURE STABILITY OF OPTIMALLY- PRASEODYMIUM-DOPED-123- $Y_{0.85}Pr_{0.15}Ba_2Cu_3O_7$ SUPERCONDUCTOR

Khaled M. Elsabawy<sup>[a,b]\*</sup> and Morsy M. Abou-Sekkina<sup>[a]</sup>

**Keywords:** Superconductor; Solution Synthesis; Visualization; X-ray; Scanning Electron Microscopy; Praseodymium-doped YBCO

The pure YBCO ( $YBa_2Cu_3O_7$ ) and optimally praseodymium containing superconductors with general formula;  $Y_{1-x}Pr_xBa_2Cu_3O_z$ , where  $x = 0.15$  mole respectively, were synthesized by solution route and characterized by XRD, SEM and Raman spectra. X-ray analyses indicated that both of pure and Pr-doped-123-YBCO has orthorhombic superconducting phase. Visualization investigations were made depending upon crystallographic data of pure and Pr-doped 123-YBCO. Both crystals are formed via DIAMOND IMPACT CRYSTAL visualizer. Comparison of structural parameters such as bond length, angles and torsion on angles of pure and Pr-doped 123-YBCO was performed to find out why this ratio of doping ( $x \sim 0.15$  mole) in most cases is reported to be optimum one in literatures.

\* Corresponding Authors

E-Mail: ksabawy@yahoo.com

[a] Chemistry Department, Faculty of Science, Tanta University- 31725-Tanta-Egypt )

[b] Faculty of Science-Chemistry Department-Taif University-Taif -Alhawayh-888-Saudi Arabia )

## Introduction

Cuprate compounds of perovskite structure have formed a big group. In recent years a research field of perovskite and related oxide materials has emerged. Because of complicated structure, it is difficult to understand the properties of cuprate. The relationship between  $T_c$  value and carrier concentration in the high  $T_c$  systems has been understood well based on an electronic phase diagram. But, the change of the carrier concentration simultaneously causes the change of the structure of the superconductors. The effect of the structural change on the  $T_c$  value has not been studied in detail. Xiao et al.<sup>1</sup> observed the existence of two subtle thermal transitions in  $YBa_2Cu_3O_{7-\delta}$  (YBCO) and the Bi-system compounds. Some workers even reported the existence of more than forty different phases in Bi-system compounds<sup>2,3</sup>. However, it is noticed that few detailed reports about the effect of Zn- and Pr-doped on the structural change of YBCO are available in literature. In the present paper, we report the subtle structural changes of the Zn- and Pr-doped YBCO, and analyze the different roles of Zn and Pr. We also suggest that the structural change has some relation with the  $T_c$  value.

The cuprate layered 123-YBCO is considered the most interesting superconducting materials for various reasons, such as their high critical temperature  $T_c$  and high critical current density  $J_c$ . Many researchers have investigated the effect of metal cation dopants on the 123-YBCO superconducting system<sup>4-8</sup>. Delamare et al.<sup>9</sup> have studied the effect of  $CeO_2$  and  $PtO_4$  mixed oxide additives on the microstructural and critical current density  $J_c$ . They reported that (Ce + Pt) oxides added to the melt-textured YBCO have significantly improved the value of  $J_c \sim 4.3 \times 10^4$  A  $cm^{-2}$ . The role of additives as impurity phases like (silver, silver oxide) to improve processing magnetization and microstructure of YBCO system was studied by many authors<sup>10-16</sup>. Tomita et al.<sup>17</sup> investigated effect of Nd-substitution partially for yttrium sites on Raman spectra of

YBCO system and reported that, Raman shifts of the vibrational modes of oxygen  $O_4$  and of the couple  $O_2-O_3$  are affected sharply by an internal pressure effect resulted from yttrium substitution.

The aim of the present work is to optimize the influence of Pr-doping ratio  $x=0.15$  mole on yttrium sites on the different structural parameters affected on lattice stability. The selected optimum Pr-doped sample was quoted from the work already done by the author himself and the selection was based on superconducting properties (best  $T_{c-offset} = 92.3$  K at  $x=0.15$  mole).

## EXPERIMENTAL

### Samples Preparation

The pure YBCO ( $YBa_2Cu_3O_7$ ) and the optimally Pr-doped YBCO superconductor with general formula;  $Y_{0.85}Pr_{0.15}Ba_2Cu_3O_7$  were prepared by solution route and sintering procedure using two different precursors.

(a) First precursor was formed from the appropriate amounts of oxides ( $Pr_2O_3 + Y_2O_3$ ) which were dissolved in few drops of concentrated nitric acid with formation of praseodymium and yttrium nitrates that finally diluted to 100 ml by distilled water and pH-adjusted to be neutral by ammonia solution.

(b) Second precursor was prepared from the appropriate amounts of  $BaCO_3$  and  $CuO$ , each of chemical grade purity with dissolution in a few drops of concentrated nitric acid, diluting the net solution to 100 ml by using distilled water and pH-adjusted to be neutral by ammonia solution.

The mixtures (a + b) were shifted to 1 L a round flask while 0.5 M urea/ $NH_3$  solution was added carefully dropwise with continuous stirring with formation of a heavy gelatinous precipitate. The precipitate were filtered off and dried, then calcinated at 850 °C under a compressed  $O_2$  atmosphere for 30 hrs, then grounded and pressed into pellets (thickness 0.2 cm and diameter 1.2 cm) under 8 Ton  $cm^{-2}$ . Sintering was carried out under oxygen stream at 940 °C for 100 h. The samples were slowly cooled down

(20 °C h<sup>-1</sup>) till 500 °C and annealed there for 25 hrs under oxygen stream. The furnace is shut off and cooled down slowly to room temperature. Finally the materials are kept in vacuum desiccator over silica gel dryer. A levitation preliminary superconductivity test was thoroughly applied for the achievement of superconductive phase and hence superconductivity.

### Phase Identification

The X-ray diffraction (XRD) measurements were carried out at room temperature on the fine ground samples using Cu-K<sub>α</sub> radiation source, Ni-filter and a computerized STOE diffractometer/Germany with two  $\theta$  step scan technique .

Scanning Electron Microscopy (SEM) measurements were carried out using a small pieces of the prepared samples by using a computerized SEM camera with elemental analyzer unit (PHILIPS-XL 30 ESEM /USA).

### Raman Spectroscopy Measurements

The measurements of Raman spectra were carried out on the finally ground powders with laser wavelength = 632.8 nm (He-Ne laser with power = 1mW) and laser power applied to the site of the sample = 0.4 mW with microscope objective = x20, accumulation time = 1000 - 4000s, up to more than an hour.

### Visualized Investigations

To visualize the praseodymium doped 123-YBCO crystal structure DIAMOND-IMPACT CRYSTAL version 3.2 GERMANY program was used depending up on the lattice coordinates given in Table.2. The visualized studies included 12 atomic parameters, 8 symmetry operation and the constructed unit cell has 14 atoms . The lattice contains (created bonds ~ 136 bonds , 8 cell corners and 12 cell edges and created atoms in it ~ 101 atoms) .

A visualized studies made is concerned by matching and comparison of experimental and theoretical data of atomic positions, bond distances, oxidation states and bond torsion on the crystal structure formed. Some of these data can be obtained free of charge from ICSD-Fiz-Karlsruhe-Germany.

## RESULTS AND DISCUSSION

### Phase Identification

Fig. 1.a and b displays the X-ray powder diffractometry patterns of pure 123-YBCO ( $YBa_2Cu_3O_7$ ) and optimally Pr-doped superconductor which prepared via solution route technique respectively. Analysis of the corresponding  $2\theta$  values and the inter-planar spacings  $d$  (Å) were carried out and indicated that the X-ray crystalline structure mainly belongs to a single superconductive orthorhombic phase 123-YBCO in major besides few peaks of  $Pr_2O_3$  as secondary phase in minor as clear (black squares) in Fig.1b. The unit cell dimensions were calculated using the most intense X-ray reflection peak and found to be  $a=3.8234$  Å,

$b=3.8662$  Å and  $c=11.7941$  Å for the pure 123-YBCO phase and  $a=3.8124$  Å,  $b=3.8532$  Å and  $c=11.8303$  Å for Pr-doped-123-YBCO. These lattice parameter values are in complete agreement with the mentioned ones in the literature.<sup>6-8</sup>

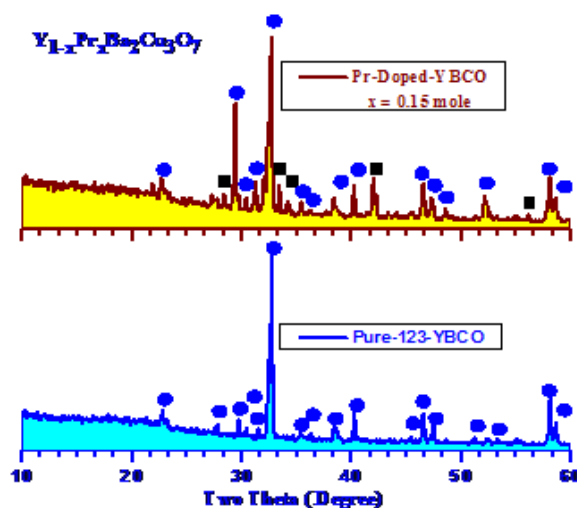


Figure 1a and b. X-ray diffraction patterns for pure YBCO and optimally doped-Pr-123-YBCO superconductors

It is obvious that, the doping with Pr-ions have a negligible effect on the main crystalline structure of the 123-YBCO regime as shown in Fig. 1a and b.

One can indicate that  $c$ -axis increases in case of optimally Pr(III) dopant concentration  $x = 0.15$  mole than the pure 123-YBCO .This is an indication for ( $Pr^{3+}$ ) ions substitute successfully by high extent in the superconductive lattice structure and cause elongation in  $c$ -axis on the basis of atomic radius since praseodymium ion is larger than that of yttrium ( $Pr^{3+} = 113$  while  $Y^{3+} = 90$  pm).

### SEM measurements

Fig. 2a and b show the SEM-micrographs for pure and optimally Pr-doped YBCO with  $x=0.15$  mole applied on the ground powders that prepared by solution route.

The average particle size was calculated and found in the range of 0.43 and 0.74  $\mu$ m. The EDX examinations for random spots in the same sample confirmed and are consistent with our XRD analysis for polycrystalline doped-YBCO composites, such that the differences in the molar ratios EDX estimated for the same sample is emphasized and an evidence for the existence of 123-YBCO superconductive phase with good approximation in contrast with real molar ratios.

From Fig.2a and b it is so difficult to observe inhomogeneity within the micrograph due to that the powders used are very fine and the particle size estimated is too small.

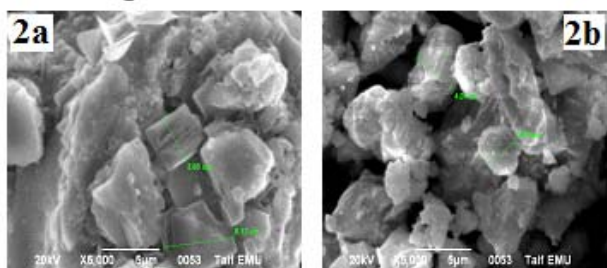


**Figure 2a and b.** SEM-micrographs recorded for pure YBCO and optimally doped-Pr-123-YBCO superconductors.

The grain size for 123-YBCO-phase was calculated according to Scherrer's formula<sup>18</sup>

$$B = 0.87 \frac{\lambda}{D \cos \theta} \quad (1)$$

where  $D$  is the crystalline grain size in nm,  $\theta$  is the half of the diffraction angle in degree,  $\lambda$  is the wavelength of X-ray source (Cu-K $\alpha$ ) in nm, and  $B$ , degree of widening of diffraction peak which is equal to the difference of full width at half maximum (FWHM) of the peak at the same diffraction angle between the measured sample and standard one. From SEM-mapping, the estimated average grain size was found to be (2.43-3.91  $\mu$ m) which is relatively large in comparison with that calculated applying Scherrer's formula for pure 123-phase ( $D \sim 1.69 \mu$ m). This indicates that, the actual grain size in the material bulk is smaller than that detected on the surface morphology. Furthermore, in our EDX (energy disperse X-ray) analysis, Pr<sup>3+</sup> was detected qualitatively with good approximate to the actual molar ratio but not observed at 123-YBCO grain boundaries which confirms that, Pr (III) has diffused regularly into material bulk of superconducting 123-YBCO-phase and Pr<sup>3+</sup>-ion induces in the crystalline structure through solid state reaction by high extent specially at optimum concentration  $x = 0.15$  mole.

**Table 1.** Mode Frequencies of Raman spectra recorded for Pr-doped-123 YBCO in the present work in contrast with some references.

References		YBCO Doping	
Ref. <sup>17</sup>	Ref. <sup>19,20</sup>	$x = 0$ mole	$x = 0.15$ mole
229	229	224.6s	223s
336	336	314m	318m
500	575	337.8m	330m
575	592	386.28b	-
440	633	438w	481m
		495.37s	580b
		571.2b	631s

s = strong, m = moderate, b = broad and w = weak.

### Raman Spectroscopy

Fig. 3a and b show the Raman spectrograms recorded for pure and optimally Pr-doped -YBCO superconductors. From the modes frequencies which are listed and compared with the work already done.<sup>18-20</sup> Table 1, one can indicate that 123-YBCO phase is the dominating phase present in

polycrystalline YBCO superconductors beside small traces of impurity phases such as unreacted praseodymium oxide in very minor traces.

From Raman spectrograms it is clear that, the fundamental vibrational modes of composites with Pr-content  $x = 0.15$  mole and pure 123-YBCO sample (Fig.3a and b) were nearly identical with those reported earlier<sup>18,19</sup> while sample with Pr-content  $x=0.15$  mole exhibited strong peak at (631  $cm^{-1}$ ) which is attributable to the impurity phase BaCuO<sub>2</sub><sup>18</sup> besides very broad line lies at  $\sim 480 \text{ cm}^{-1}$  that appears also in pure sample but shifting by  $\pm 10 \text{ cm}^{-1}$  may be attributable to praseodymium(III) ions interactions make as raman scattering materials with other different M-O vibrational modes.

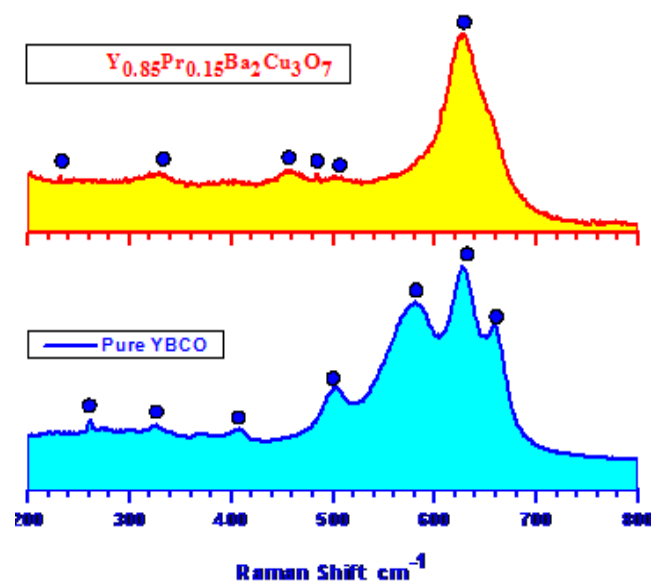


**Figure 3a and b.** Raman spectrograph recorded for pure YBCO and optimally doped-Pr-123-YBCO superconductors.

The vibrational Raman active-phonon mode lies at  $\sim 480 \pm 10 \text{ cm}^{-1}$  originally is due to the apical oxygen O4 ( $A_{1g}$ )<sup>18</sup>. This vibrating mode became flat and very broad to be noticeable in the YBCO-composites with  $x = 0.15$  mole. This flattening is attributed to disturbances and changes occurred in the inter-atomic distances of apical oxygen O4 to the two copper layers (Cu2) whereas Pr<sup>3+</sup> substitutes Y-sites by high extent at low concentration optimum doping ratio ( $x = 0.15$  mole) and as a result O4-Cu2 interatomic distances became more closer. In addition to a disorder is occurred on the Cu-O chain which is due to oxygen deficiency on the 123-YBCO lattice structure. Further more Pr<sub>2</sub>O<sub>3</sub> which appears as impurity phase as confirmed in our X-ray measurements Fig.1b can play as strong raman scattering material<sup>19</sup>.

It is known that the vibrational mode lies at  $330 \pm 10 \text{ cm}^{-1}$  is the out-of-phase  $B_{1g}$  of the couple O<sub>2</sub>-O<sub>3</sub> which in our results strongly shifted down due to Pr-ions substitutions.

According to results reported by Thomsen et al.<sup>22</sup> the two lines lie at 224 and  $570 \pm 10 \text{ cm}^{-1}$  (which in our results shifted down  $\sim 10\text{-}20 \text{ cm}^{-1}$ ) have been identified as the

**Table 2:** Lattice coordinates data of Pr-doped-YBCO.

Atomic parameters							
Atom	Ox.	Wyck.	Site	S.O.F.	x/a	y/b	z/c
Ba1		2t	mm2	0.99	1/2	1/2	0.18200
Y1		2t	mm2	0.005	1/2	1/2	0.18200
Pr1		2t	mm2	0.005	1/2	1/2	0.18200
Y2		1h	mmm	0.850	1/2	1/2	1/2
Pr2		1h	mmm	0.150	1/2	1/2	1/2
Cu1		1a	mmm	1.00	0	0	0
Cu2		2q	mm2	1.00	0	0	0.35000
O1		1b	mmm	0.03	1/2	0	0
O2		1e	mmm	0.97	0	1/2	0
O3		2r	mm2	1.00	0	1/2	0.19500
O4		2r	mm2	1.00	0	1/2	0.37200
O5		2s	mm2	1.00	1/2	0	0.39400

forbidden vibration modes of copper and oxygen in the Cu-O chain layer respectively. Based on the selection rules generally these modes are forbidden in case of samples having sufficient oxygen content.

Duong et al.<sup>18</sup> confirmed that when the number of oxygen atoms in the unit cell is  $< 7$ , the CuO chain could start to become disordered and its inversion center of symmetry is broken and then the mentioned two lines (at 229 and 567  $\text{cm}^{-1}$ ) can appear.

Regarding these informations reported<sup>22,18</sup> present results are partially agreement and consistent with them since the optimally Pr-doped sample displays two lines with different intensities as per the oxygen content inside lattice. From Fig.3a and b one can notice that there is no monotonic behaviour on the recorded Raman spectrograph due to high sensitivity of both 123-YBCO systems and Raman spectra favour applicable variables, such as structure quality which depends upon oxygen content and impurity phases. All of these variables can make a change on the Raman phonon modes as mentioned in literature before. Figure 4a. Orthorhombic crystal structure of Pr-optimally doped-123-YBCO superconductor.

### Structural Visualization

The pure crystal and praseodymium doped crystal were built up depending upon the atomic parameters and lattice coordinates in Table 2 with the help of DIAMOND visualizer and can be seen at Figs. 4a-c. The comparison between fingerprint peaks in Fig.1a and b and theoretical XRD-pattern Fig.4b indicated that there are good fitting between both the patterns which reflect the success of praseodymium doping ( $x=0.15$  mole) to substitutes without distorting the original orthorhombic structure. It is well known fact that superconduction mechanisms inside these cuprates layered structures are mainly depend upon Cu-O chains and planes as shown in Fig.4c. Furthermore any kind of shortening or lengthening in these (chains and planes) could damage superconductivity nature inside these superconductors<sup>2,3,4</sup>.

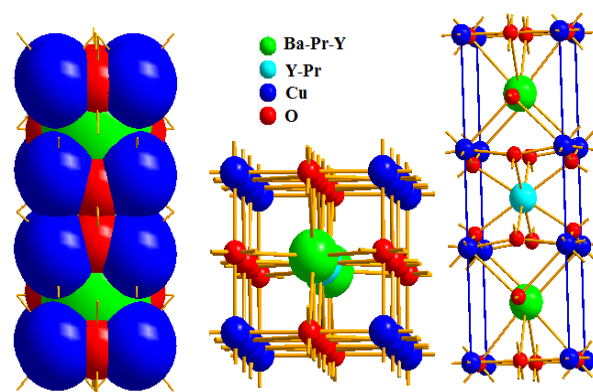


**Figure 4a.** Orthorhombic crystal structure of Pr-optimally doped-123-YBCO superconductor.

So a visualized studies made is concerned by matching and comparing of experimental and theoretical data of atomic positions, bond distances, oxidation states and bond torsion on the crystal structure formed.

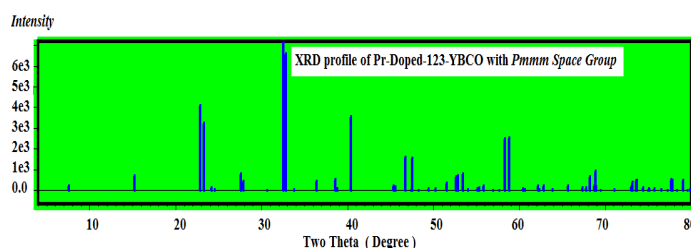


**Figure 4b.** Visualized XRD-profile recorded for Pr-optimally-doped-123-YBCO.

The analysis of tables (3, 4 and 5) indicated that there is no violation in bond lengths especially for praseodymium-oxygen since praseodymium found in two types symbolized as Pr1 and Pr2 respectively.

It was noticed that Pr1 linked with five types of oxygen atoms namely O1, O2, O3, O4 and O5 recording the following bond lengths 2.8763, 2.8551, 1.9165, 2.9251 and 3.1432 Å respectively.

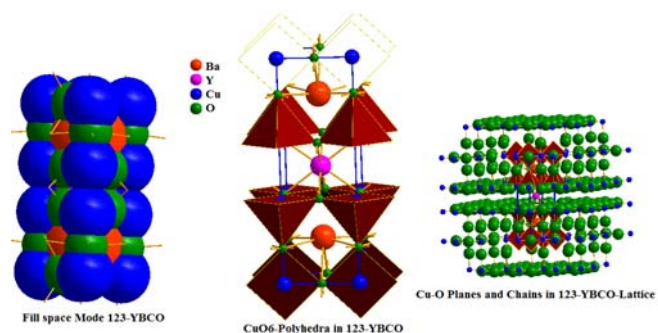


**Figure 4c.** Copper–oxygen planes and chains and  $CuO_6$ -poly octahedrons.

These recorded data for type one are slightly different from those of type two (Pr2) which linked with  $O_5$  and  $O_4$  and recording 2.3018 and 2.4242 Å respectively. The differences in bond lengths could be interpreted on the basis that Pr-ions have more than one oxidation state inside crystal lattice. With respect to stability of  $CuO_6$  polyhedrons inside the optimally-Pr-doped YBCO crystal lattice, it was observed that bond distances between copper and oxygen atoms environment are within the limits and no violation was recorded except only in  $Cu1-O5$  is longer than others due to axial positioning of  $O5$ . Furthermore, no abnormal torsions observed on the angles of copper which support and increase stability of lattice.

**Table 3.** Some selected structural data inside crystal lattice of Pr-doped-YBCO.

Atom1	Atom2	$d_{1-2}$ Å	Atom3	$d_{1-3}$ Å	$\wedge 213^\circ$
Ba1 Pr1 Y1	O3	1.9165	O3	1.9165	170.929
	O3	1.9165	O2	2.8551	136.537
	O3	1.9165	O2	2.8551	52.535
	O3	1.9165	O1	2.8763	93.344
	O3	1.9165	Ba1 Pr1 Y1	3.8840	90.000
	O3	1.9165	Ba1 Pr1 Y1	3.8840	90.000
	O3	1.9165	O2	2.8551	52.535
	O3	1.9165	Cu1	3.4530	59.804
	O3	1.9165	Y2 Pr2	3.7072	85.464
	O3	1.9165	Ba1 Pr1 Y1	3.8210	4.536
	O3	1.9165	Ba1 Pr1 Y1	3.8210	175.464
	O3	1.9165	Ba1 Pr1 Y1	3.8840	90.000
	O2	2.8551	Cu1	3.4530	85.043
	O2	2.8551	Cu1	3.4530	34.223
	O2	2.8551	Y2 Pr2	3.7072	137.999
	O2	2.8551	Ba1 Pr1 Y1	3.8210	47.999
	O2	2.8551	Ba1 Pr1 Y1	3.8210	132.001
	O2	2.8551	Ba1 Pr1 Y1	3.8840	90.000
	O2	2.8551	Ba1 Pr1 Y1	3.8840	90.000
	O2	2.8551	Ba1 Pr1 Y1	3.8840	90.000
	O1	2.8763	O1	2.8763	84.934
	O1	2.8763	O4	2.9251	123.958
	O1	2.8763	O4	2.9251	123.958
	O1	2.8763	O5	3.1432	175.692
	O1	2.8763	O5	3.1432	99.374
	O1	2.8763	Cu2	3.3552	145.224
	O1	2.8763	Cu2	3.3552	145.224
	O1	2.8763	Cu2	3.3552	92.282
	O4	2.9251	Cu2	3.3552	35.518
	O4	2.9251	Cu2	3.3552	35.518
	O4	2.9251	Cu2	3.3552	85.979
	O4	2.9251	Cu1	3.4530	145.758
	O4	2.9251	Cu1	3.4530	95.965
	O4	2.9251	Cu1	3.4530	145.758
	O4	2.9251	Cu1	3.4530	95.965
	O5	3.1432	Cu1	3.4530	146.164
	O5	3.1432	Cu1	3.4530	97.798
	O5	3.1432	Y2 Pr2	3.7072	38.159
	O5	3.1432	Ba1 Pr1 Y1	3.8210	90.000
	O5	3.1432	Ba1 Pr1 Y1	3.8210	90.000
	O5	3.1432	Ba1 Pr1 Y1	3.8840	128.159
	O5	3.1432	Ba1 Pr1 Y1	3.8840	51.841
	O5	3.1432	Cu2	3.3552	84.181
	O5	3.1432	Cu2	3.3552	84.181

**Table 4.** Selected structural data inside crystal lattice of Pr-doped-YBCO.

Atom1	Atom2	$d_{1,2}$ Å	Atom3	$d_{1,3}$ Å	$\angle 213^\circ$
Y2 Pr2	O5	2.3018	O5	2.3018	180.000
	O5	2.3018	O5	2.3018	64.939
	O5	2.3018	O5	2.3018	115.061
	O5	2.3018	Cu2	3.2372	102.481
	O5	2.3018	Cu2	3.2372	102.481
	O5	2.3018	Cu2	3.2372	37.238
	O5	2.3018	Cu2	3.2372	37.238
	O5	2.3018	Ba1 Pr1 Y1	3.7072	57.530
	O5	2.3018	Ba1 Pr1 Y1	3.7072	122.470
	O5	2.3018	Y2 Pr2	3.8210	90.000
	O5	2.3018	Y2 Pr2	3.8210	90.000
	O4	2.4242	Cu2	3.2372	37.096
	O4	2.4242	Ba1 Pr1 Y1	3.7072	127.992
	O4	2.4242	Ba1 Pr1 Y1	3.7072	52.008
	O4	2.4242	Y2 Pr2	3.8210	37.992
	O4	2.4242	Y2 Pr2	3.8210	142.008
	O4	2.4242	Ba1 Pr1 Y1	3.7072	52.008
	O4	2.4242	Ba1 Pr1 Y1	3.7072	127.992
	O4	2.4242	Y2 Pr2	3.8210	142.008
	O4	2.4242	Y2 Pr2	3.8210	37.992
	O4	2.4242	Y2 Pr2	3.8840	90.000
	O4	2.4242	Y2 Pr2	3.8840	90.000
	O4	2.4242	Y2 Pr2	3.8840	90.000
	O4	2.4242	Y2 Pr2	3.8840	90.000
	O4	2.4242	Y2 Pr2	3.8840	90.000
	Cu2	3.2372	Cu2	3.2372	72.339
	Cu2	3.2372	Cu2	3.2372	114.607
	Cu2	3.2372	Cu2	3.2372	73.726
	Cu2	3.2372	Cu2	3.2372	106.274
	Cu2	3.2372	Y2 Pr2	3.8210	126.169
	Cu2	3.2372	Y2 Pr2	3.8840	53.137
	Cu2	3.2372	Y2 Pr2	3.8840	126.863
	Ba1 Pr1 Y1	3.7072	Ba1 Pr1 Y1	3.7072	180.000
	Ba1 Pr1 Y1	3.7072	Y2 Pr2	3.8210	90.000
	Ba1 Pr1 Y1	3.7072	Y2 Pr2	3.8210	90.000
	Ba1 Pr1 Y1	3.7072	Y2 Pr2	3.8840	90.000
	Y2 Pr2	3.8210	Y2 Pr2	3.8210	180.000
	Y2 Pr2	3.8210	Y2 Pr2	3.8840	90.000
	Y2 Pr2	3.8210	Y2 Pr2	3.8840	90.000

**Table 5.** Selected structural data inside crystal lattice of Pr-doped-YBCO.

Atom1	Atom2	$d_{1,2}$ Å	Atom3	$d_{1,3}$ Å	$\angle 213^\circ$
Cu1	O1	1.9105	O1	1.9105	180.000
	O1	1.9105	O2	1.9420	90.000
	O1	1.9105	O2	1.9420	90.000
	O1	1.9105	O3	2.9899	90.000
	O1	1.9105	Ba1 Pr1 Y1	3.4530	56.407
	O1	1.9105	O2	1.9420	90.000
	O1	1.9105	O3	2.9899	90.000
	O1	1.9105	Cu1	3.8840	90.000
	O2	1.9420	Ba1 Pr1 Y1	3.4530	124.223
	O2	1.9420	Cu1	3.8210	90.000
	O2	1.9420	Cu1	3.8210	90.000
	O2	1.9420	Cu1	3.8840	0.000
	O2	1.9420	Cu1	3.8840	180.000
	O2	1.9420	O3	2.9899	130.506
	O2	1.9420	Ba1 Pr1 Y1	3.4530	124.223
	O3	2.9899	O3	2.9899	81.012
	O3	2.9899	O3	2.9899	98.988
	O3	2.9899	O3	2.9899	180.000

**Table 5 (cont.).** Selected structural data inside crystal lattice of Pr-doped-YBCO.

Atom1	Atom2	$d_{1,2}$ Å	Atom3	$d_{1,3}$ Å	$\wedge 213^\circ$
Cu1	O3	2.9899	Ba1 Pr1 Y1	3.4530	146.357
	O3	2.9899	Cu1	3.8840	49.494
	O3	2.9899	Cu1	3.8840	130.506
	O3	2.9899	Ba1 Pr1 Y1	3.4530	33.643
	O3	2.9899	Ba1 Pr1 Y1	3.4530	84.151
	Ba1 Pr1 Y1	3.4530	Ba1 Pr1 Y1	3.4530	75.826
	Ba1 Pr1 Y1	3.4530	Ba1 Pr1 Y1	3.4530	180.000
	Ba1 Pr1 Y1	3.4530	Ba1 Pr1 Y1	3.4530	67.186
	Ba1 Pr1 Y1	3.4530	Cu1	3.8840	124.223
	Ba1 Pr1 Y1	3.4530	Cu1	3.8840	55.777
	Cu1	3.8210	Cu1	3.8210	180.000
	Cu1	3.8210	Cu1	3.8840	90.000
	Cu1	3.8210	Cu1	3.8840	90.000
	Cu1	3.8210	Cu1	3.8840	90.000
	Cu1	3.8210	Cu1	3.8840	90.000

## Conclusions

The conclusive remarks regarding this article can be summarized in the following points;

Doping with Pr-ions at optimal ratio have a negligible effect on the main crystalline structure of the 123-YBCO regime ( $x = 0.15$  mole).

The average particle size was calculated and found in the range of 0.43 and 0.74  $\mu\text{m}$ .

The vibrational mode lies at  $330 \pm 10 \text{ cm}^{-1}$  is the out-of-phase  $B_{1g}$  of the couple O2-O3 which in present investigations strongly shifted down with Pr- doping  $x=0.15$  mole.

Structural visualization studies confirmed that Pr-doping with optimal ratio  $x=0.15$  mole reinforces the stability of 123-YBCO lattice structure .

## Acknowledgement

The authors would like to thank deeply JANSEN Department represented by Prof. M.Jansen (Max Planck Institute for Solid State Research-1-D-Heissenberg Str. - Stuttgart-Germany) for their technical support of some measurements inside this article.

## References

- Xiao, G., Streitz, F. H., Gavrin, A., Du, Y. W., Chien, C. L., *Phys. Rev. B*, **1987**, 35, 8782.
- Maeno, Y., Tomita, T., Kyogoku, M., Aoki, Y., Hoshino, K., Minami, A., Fujita, T., *Nature*, **1987**, 328, 512 .
- Tarascon, J. M., Barboux, P., Maceli, P. F., Greene, L. H., Hull G. W., *Phys.Rev. B*, **1988**, 37, 7458.
- Renevier, H., Hodeau, J. L., Marezio, M., Santoro, A., *Physica C*, **1994**, 220, 143 .
- Kulkarni, R. G., Kuberkar, D. G., Baldaha, G. J., Bichile, G. K., *Physica C*, **1993**, 217, 175.
- Bringley, J. F., Chen, T. M., Averill, B. A., Wong K. M., Poon, S. J., *Phys. Rev.B*, **1988**, 38, 2432.
- Shimak, Y. A., Kubo Y., Utsumi, K., Takeda, Y., Takano, M., *Jpn. J. Appl. Phys.*, **1988**, 27, 1071 .
- Hiroi, Z. , Takano, M., Takeda, Y., Kanno, R., Bando, Y., *Jpn. J. Appl. Phys.*, **1988**, 27, 580 .
- Delamare, M. P., Hervieu M., Monot I and Tendeloo G., *Physica C*, **1996**, 262, 220.
- Peters, P. N., Sisk, R. C., Ubran, E., Huang, C. Y., Wu M. K., *Appl. Phys. Lett.*, **1988**, 52, 2066 .
- Huang, C. Y., Shapiro, Y., McNiff, E. J., Peters, P. N., Shwartz B. B., Wu, M. K., Shull, R. D., Chiang, C. K., *Mod. Phys.Lett.*, **1988**, 2, 869.
- Singh J. P., Leu, H. L., Poepple, R. B., Voorhees, E., Goudery, G. T., Winsley, K., Shi, D., *J. Appl. Phys.*, **1989**, 66, 3154.
- Dwir, B., Affronte, M. and Pavuna, D., *Appl. Phys. Lett.*, **1989**, 55, 399.
- Jung, J., Mohammed, M. A., Cheng, S. C., Frank, J. P., *Phys. Rev. B*, **1990**, 42, 6181.
- Singh, J. Joo, J. P., Gangopadhyay, A. K., Mason, T. O., *J. Appl. Phys.*, **1992**, 71, 2351.
- Khan, H. R., Fancavilla, T. L., Hein, R. A., Pande, C. S., Quadri S. B., Soulen, R. J., Wolf, S. A., *J. Supercond.*, **1990**, 3, 189.
- Tomita, M. and Murakami M., *Supercond.Sci. Technol.*, **2000**, 13, 722 .
- Duong, C. H. , Vu, L. D. and Hong, L.V., *J. Raman Spectrosc.*, **2001**, 32, 827.
- Zhang, L. D. , Mu, J. M., Nano-materials Science, *Liaoning Science & Technology Press*, Shengyan, China, **1994**, p. 92.
- Kaihana, M., Borjesson, L., Eriksson, S., *Physica C*, **1989**, 162, 1253.
- Chang, H., Ren, Y., Sun, Y., Wang, Q., Xue, Y., Chu C. W., *Physica C*, **1994**, 228, 383 .
- Thomsen, C., Cardona, M., Gegenheimer, B., Lui, R., Simon, A., *Phys. Rev. B*, **1988**, 37, 284.

<sup>23</sup>Sekkina M. M. A., Elsabawy, K. M., *Mater. Sci. Eng.*, **2003**, B103, 71-76.

<sup>24</sup>Elsabawy, K. M., Elsayed, K. E., *Mater. Res. Bull.*, **2007**, 42, 1051-1060.

Received: 20.10.2012.

Accepted: 13.11.2012.